International Journal of Thermophysics, Vol. 14, No. 3, 1993

Thermophysical Properties of Solid and Liquid Beryllium[1]

M. Boivineau,[2] L. Arlès,[2] J. M. Vermeulen,[2] and Th. Thévenin[2]

A submillisecond resistive heating technique under high pressure (0.12 GPa) has been used to measure selected thermophysical properties of both solid and liquid beryllium. Data have been obtained between room temperature and 2900 K. Results on enthalpy, volume expansion, electrical resistivity, and sound velocity measurements are presented.

KEY WORDS: beryllium; electrical resistivity; enthalpy; high pressure; high temperature; isobaric expansion; liquid metals; sound velocity.

1. INTRODUCTION

The physical properties of beryllium are of interest because of its numerous applications in different areas of technology and science, such as aerospace and nuclear reactors. Furthermore, this material presents an atypical behavior related to extreme chemical and thermophysical properties. Indeed, beryllium exhibits unusual high values of specific heat, electrical and thermal conductivities, Debye temperature (1463 K), sound velocity ($\approx 13{,}000\ \mathrm{m \cdot s^{-1}}$ at 300 K), and consequently elastic moduli [1]. For example, its high Young's modulus ($E \approx 300$ GPa at 300 K), correlated to a high rigidity, is about one and one-half times that of an austenitic stainless steel and four times that of aluminium. The low density of beryllium leads to an unsurpassed specific elastic modulus E/ρ value. Moreover, this element has a very low Poisson's coefficient (0.02 to 0.04, compared with the 0.2 to 0.3 usual values for other metals) and thus a high

[1] Paper presented at the Third Workshop on Subsecond Thermophysics, September 17–18, 1992, Graz, Austria.

[2] Commissariat à l'Énergie Atomique, Centre d'Études de Bruyères-le-Châtel, BP 12, F-91680 Bruyères-le-Châtel, France.

0195-928X/93/0500-0427$07.00/0

resistance to the lateral contraction. Its metallurgy also presents some unusual features [2] since, on one hand, there is a large entropy difference at the α–β transition in the solid state occurring at about 1530 K and ambient pressure and, on the other hand, the β phase exists only for a very small temperature range since beryllium melts at about 1560 K. The α phase, existing at room temperature and ambient pressure, crystallizes in the hexagonal close-packed structure (hcp) and has a c/a ratio (1.568) which is the lowest among the isomorphic metals. Such a fact enhances the stability of this hexagonal structure and leads to a marked anisotropy. Before melting at 1560 K, Be transforms into the body-centered cubic structure (bcc) for the β phase.

At present, a significant number of data are available for solid Be for various purities [2–4], whereas only a few are reported in the literature for the liquid state. In the present paper, we focus our attention particularly on measurements in the liquid phase.

A submillisecond-resolution dynamic heating technique, pioneered by Levedev et al. [5], and called isobaric expansion experiment (IEX) by Gathers et al. [6], has been used successfully to study both solid and liquid states of beryllium. This kind of pulse heating technique, compared with conventional static ones, has the advantage of reducing chemical reactions between the sample and its environment and of significantly lowering radiative heat losses and hydrodynamic instabilities. Moreover, gravity effects on the sample can be neglected once the sample is in its liquid state.

As described later, this experiment leads to basic thermophysical properties which are necessary to complete data for fluid metal models, to determine equation-of-state parameters, and to adjust calculations on liquid metals. In this paper, we present the results on enthalpy, volume expansion, electrical resistivity, and sound velocity measurements for solid and liquid beryllium.

2. EXPERIMENTAL TECHNIQUE

Our technique, described in detail elsewhere [7], consists in resistively pulse heating metallic cylindrical samples (0.8×30 mm for beryllium) by discharging a 60-kJ capacitor bank (20 kV, 300 μF) in about 100 μs. The sample container consists of an argon gas-filled high pressure cell.

This experiment gives access to different measured values such as voltage drop across a known length of the sample, current through the sample, pressure of the environment, radial expansion, thermal radiation from the heated sample (multichannel pyrometric technique), and sound velocity. From these data, it is then possible to deduce other quantities such as enthalpy (defined as the time integral of the measured current times the

voltage per unit mass), temperature, volume expansion, volume-corrected electrical resistivity, heat of phase transformation, and specific heat at constant pressure. Except for the sound velocity, all the measured data are function of time and can be then all combined together.

Sound velocity data are also very useful since they lead to the equation-of-state parameters of the material, such as the isothermal and adiabatic bulk moduli and compressibilities, the ratio of specific heats, and the Grüneisen parameter. Thus, the latter may be expressed from the knowledge of the sound velocity c by the following relation:

$$\gamma_G = \beta \frac{c^2}{C_p} \tag{1}$$

where β is the volume expansion coefficient and C_p is the specific heat at constant pressure. Both are calculated by derivating the specific volume-versus-temperature and enthalpy-versus-temperature curves, respectively.

Since C_p and β are independent of temperature and constant in the liquid state, this parameter is thus only proportional to the square of the sound velocity. The ratio of specific heats, defined as $\gamma = C_p/C_v$, may also be determined from

$$\gamma = 1 + \beta T \gamma_G \tag{2}$$

The adiabatic bulk modulus B_S is related to the sound velocity and the density ρ by the following equation:

$$B_S = V\left(\frac{\partial P}{\partial V}\right)_S = \rho c^2 \tag{3}$$

It is then easy to deduce the adiabatic compressibility from

$$K_S = \frac{1}{B_S} \tag{4}$$

The isothermal bulk modulus B_T or compressibility K_T may be found in the same manner since

$$B_T = V\left(\frac{\partial P}{\partial V}\right)_T = \frac{B_S}{\gamma} \tag{5}$$

and

$$K_T = \frac{1}{B_T} \tag{6}$$

The above equations show the importance of sound velocity measurements in this experiment. Since the sample stays in its equilibrium state at any time of the experiment and by overcoming contamination problems, it is then possible to measure equation-of-state parameters to much higher temperatures compared with static techniques.

All the experiments have been here performed under a 0.12-GPa argon pressure. It is preferred to keep the pressure constant for the following reasons. (i) It is placed inside the cell to avoid refraction effects, to obtain a better image resolution, and to collect more light from the sample. Its performances and characteristics are predefined because the argon refractive index notably depends on pressure. Hence, one needs to change the optics or its position inside the chamber for different pressures. (ii) The quality and the sharpness of the sound velocity streaking photograph are very sensitive to pressure and thus impose to work in a very short range (± 5 MPa) around the chosen pressure value. Sapphire windows are used to resist to high pressures up to 0.6 GPa and to give access to optical measurements such as backlighting and pyrometric techniques.

As described by Berthault et al. [7], volume expansion measurements are obtained by coupling a shadowgraph technique with a high-speed image converter streak camera. Temperature measurements are performed using a four-channel pyrometer. This latter has the main drawback of being incompatible with sound velocity measurements since one needs high reflection coefficient optics to reach the pyrometer's threshold (≈ 1600 K). Thus, so far, we are not able to see the melting plateau for elements presenting a low melting point. Then our temperature scale often comes from the combination of the C_p data reported in the literature and our experimental enthalpy data.

This IEX has been improved by developing a sound velocity measurement system to extend its own experimental capabilities. The basic principle is similar to those of Gathers et al. [8] and Hixson et al. [9] and has been successfully applied in our laboratory for several years. It consists of generating a stress pulse by focusing a Q-switched laser on the sample. Such a stress wave is spherically diverging and converts into an acoustic wave when crossing the sample.

This technique, pioneered by Brammer and Percival [10], has received a great deal of attention for numerous applications such as nondestructive testing and transducer characterization. Calder and Wilcox [11] improved and applied this technique to the measurements of elastic constants for the IEX [8]. The fundamental process which initiate the generation of acoustic waves or other thermoelastic effects by modulated optical radiation have been reviewed in detail by Tam [12].

The acoustic modes generated by laser pulses are produced in two

principal ways: the thermoelastic regime, operating at low energy levels, and the ablation process, occurring at higher laser powers. Both processes may be described as follows. (i) The very fast heating (≈ 10 ns) of a thin sample surface created by the laser pulse produces a thermal expansion which works against the sample inertia, then generating a constraint at the border of the heated area which leads to elastic waves: this is the thermoelastic regime. Such a mechanism corresponds to the formation of thermal gradients, and the resulting longitudinal (atom motion parallel to the propagation direction) or shear (atom motion perpendicular to the propagation direction) waves are proportional to the laser energy for the same pulse duration and focal spot size [13, 14]. (ii) When the absorbed laser light is high enough to bring a thin depth of the material up to the boiling state, the recoil energy generated by the vaporized atoms initiates elastic waves: this is the ablation regime.

For this experiment, a low-energy level TEM_{00} Q-switched ruby laser (25 mJ, 10 ns) is focused on the sample with an irradiated surface corresponding to a focal spot diameter of about 180 μm. In that case, the thermoelastic regime should be dominant to produce elastic waves.

Using a shadowgraph technique, one can observe on a streak camera a disturbance in the surrounding argon which propagates outward from the side opposite the ruby laser focal point. This disturbance, associated with the stress wave path into the argon, is characterized by a shadow in the illuminated surrounding gas and is caused by the resulting acoustic index of the refraction gradient (propagating at the acoustic velocity) produced by the thermal gradient. It is then possible to follow this shadow, particularly back to its starting point from the sample surface (opposite to the source), which corresponds to the transit time of the sound wave after crossing the sample. Thus, it is easy to deduce the sound velocity value of the material since the diameter of the sample at the ruby laser pulse time (stress pulse time) is known. The latter is calculated from radial expansion data obtained with a streak camera (Thomson-CSF Model TSN503) operating during a 200-μs time. To obtain precise measurements on the transit time of the acoustic wave across the sample and then to reduce errors on sound velocity data, one must change the streak duration. This is done by using another camera (Hadland Model Imacon 790) whose 3.5-μs streak duration, correlated to a streaking velocity of 50 ns $\cdot$ mm^{-1}, is used for the present study since the beryllium has a very high sound velocity value ($\approx 13{,}000$ m $\cdot$ s^{-1} at 300 K). The camera is triggered when the ruby laser pulse occurs. We should mention that the ruby laser also causes a disturbance on the sample shadowgraph which is easily recognizable and thus simplifies the sound velocity transit time measurements on the streak photograph. The laser is triggered after heating has

been stopped and when the sample is in an equilibrium end state in its liquid phase.

One of the main advantages of this method is its ease to perform compared with the interferometric method has the principal drawback of being very sensitive to sample motions during the heating process.

Furthermore, this configuration gives access only to the longitudinal velocity measurement. Assumptions are thus necessary to calculate the elastic moduli in the solid state since both longitudinal and shear modes occur, the latter being nonexistent in the liquid phase.

The estimated error of the sound velocity measurements in this experiment has been in the ± 5–10% range. These experimental uncertainties depend mainly on the quality of the streaking photograph to measure the transit time of the acoustic wave crossing the sample and on the determination of the sample diameter at the laser pulse time.

3. RESULTS

Three kinds of materials coming from different origins have been tested since we have encountered numerous problems in performing this experiment. The samples we used are S200F (batch 3976 S/N 5), SRH (batch 2574), and S65 (batch 870513). The S200F (Brush Wellman) and SRH (Pechiney) samples are received in our laboratory in the form of massive samples. As expected, the SRH samples are very pure since the total metallic impurities are equal to 80 ppm, by weight, compared with 1880 ppm, by weight, for the S200F samples. Note that for both, the concentration of carbon is about 1000 ppm, by weight. The S65 samples are received in powder form and then undergo different specific treatments performed in Bruyères-le-Châtel [15].

The SRH samples were prepared by casting before being extruded, whereas the S200F and S65 samples, extracted from powder metallurgy processes, were obtained by unidirectionnal hot pressing (HP) and hot isostatic pressing (HIP), respectively. The latter two processes consist of inserting under vaccum the beryllium powder in water-tight sheaths and then bringing them up to high temperature and pressure values. The sintering mechanism is thus accelerated and leads to the densification of the material for values of about 1300 K and 100 MPa. All the samples (including the SRH ones) are then dry machine turned to their final shape.

The most important problem we met was a nearly systematic unseasonable vaporization of the S200F and SRH samples without reaching the liquid state. This is why there are fewer points for this phase in Fig. 3 compared with solid beryllium. This problem has been partially overcome by using S65 samples which are outgassed and thermally treated

[15]. Indeed, these S65 samples have led to better results in terms of reproductibility since the liquid state has always been reached.

Another drawback of beryllium is that it is fragile, which leads to difficulties in setting up the sample in the experimental chamber. We also have encountered problems of contact losses and observed hazy shadow contours on the expansion image.

It is also known that beryllium properties, such as mechanical characteristics, electrical resistivity, thermal expansion, and specific heat, are very sensitive to impurities and lattice effects (textured materials) and, thus, to the metallurgical treatment of the material [2, 4, 16]. Great care must be taken to prepare the sample and to compare results on samples which are initially different. As shown later, such variations seem to be confirmed on the sound velocity measurements.

The thermophysical properties of a S65 beryllium sample are presented in Table I. All values were obtained under 0.12-GPa pressure. The V_0 value is referred to 300 K, i.e., $5.405 \times 10^{-4}\ m^3 \cdot kg^{-1}$, and the electrical resistivity data are volume corrected.

Since our pyrometers work only over a high temperature range with the use of logarithmic amplifiers and because of their incompatibility with sound velocity measurements (see above), temperature values are obtained from C_p static data given in the literature [17].

The relative volume versus enthalpy is shown in Fig. 1. Such a curve

Table I. Thermophysical Properties of Solid and Liquid Beryllium at $P = 0.12$ GPa

H (MJ · kg^{-1})	T (K)	ρ_{el} ($\mu\Omega \cdot$ cm)	V/V_0
0.00	293	4.6	1
0.50	525	11.2	1.01
1.00	718	18.5	1.028
1.50	896	26.5	1.065
2.00	1060	37.4	1.127
2.50	1217	50.4	1.163
3.00	1364	66.3	1.188
3.50	1505	88.9	1.207
3.71 (s)	1564	110.4	1.212
4.01	1564	128.8	1.23
4.50	1564	155.2	1.253
4.85 (l)	1564	161.9	1.264
5.00	1607	164.2	1.270
5.51	1762	165.4	1.290
6.00	1908	165.5	1.314
6.51	2062	165.7	1.343

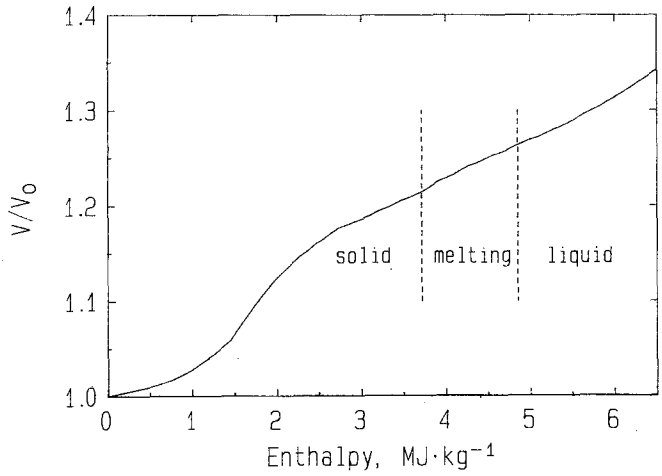

Fig. 1. Relative volume V/V_0 plotted against enthalpy for beryllium.

is obtained since one knows the sample diameter, the voltage, and the current measurements, all of them being a function of time. However, one should note that the specific volume varies significantly from one shot to another for the case of beryllium. For this purpose, we already mentioned the problems of hazy contours resulting in the observation of disturbances or lumpy edges on the expansion images. Such disturbances might be explained by the development of hydromagnetic instabilities, which should be more pronounced for low-density and high-conductivity metals [18]. Consequently, this leads to higher error estimates on the volume measurements, whose expected value is typically $\pm 2\%$ [7]. This value can reach ± 4–5% or even more in some cases. Figure 1 presents one of the best shots, where no disturbance was observed. In this case, the accuracy is found to be about $\pm 2\%$.

The best fit to the volume data in Fig. 1 in the solid phase is given by

$$V/V_0 = 1.004 - 2.6 \times 10^{-2} H + 6.5 \times 10^{-2} H^2 - 1.1175 \times 10^{-2} H^3 \quad (7)$$

for $0 \leqslant H \leqslant 3.71$ MJ $\cdot$ kg^{-1}. In the liquid phase, we find a best fit of

$$V/V_0 = 1.2845 - 4.3 \times 10^{-2} H + 8 \times 10^{-3} H^2 \quad (8)$$

for $4.85 \leqslant H \leqslant 6.5$ MJ $\cdot$ kg^{-1}.

In Fig. 2, the resistivity values of the same sample (S65) are plotted against enthalpy with and without volume correction. Because of the lack of information concerning the liquid state, we have not been able to

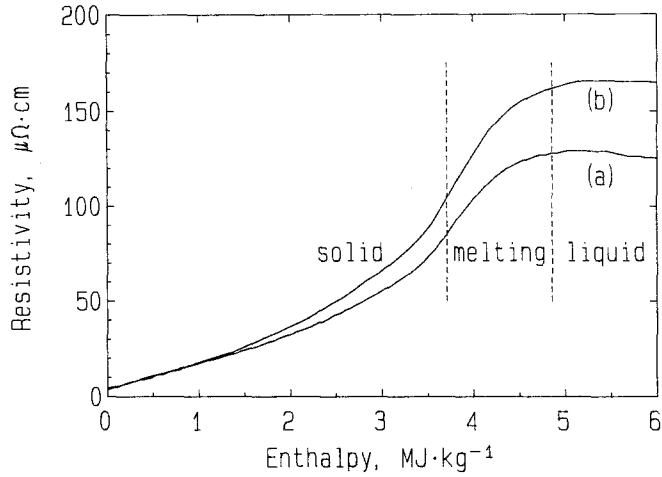

Fig. 2. Electrical resistivity-versus-enthalpy data for beryllium: (a) without volume correction; (b) with volume correction.

compare our results with data in the literature. However, it may be noted that the value of 4.6 $\mu\Omega \cdot$ cm for the resistivity value at 300 K (see Table I) is in good agreement with the data reported in the literature in the 4.26–5.5 $\mu\Omega \cdot$ cm range [2]. These data come from the Brush Beryllium Company, whose aim was to study the effects of impurities on the mechanical properties of beryllium. We also have observed differences in resistivity values for different samples since their variation is in the 4.2–5.0 $\mu\Omega \cdot$ cm range. From our results, the density seems to decrease with the degree of purity, the S200F and SRH samples giving the highest and lowest values, respectively.

The best polynomial fit to the corrected resistivity data in the solid state is given by

$$\rho_{el} = 4.0 + 15.9H - 2.613H^2 + 1.446H^3 \tag{9}$$

for $0 \leqslant H \leqslant 3.71$ MJ $\cdot$ kg^{-1}, and where ρ_{el} is in $\mu\Omega \cdot$ cm. In the liquid phase, the corrected resistivity remains constant at an average value of 165.5 $\mu\Omega \cdot$ cm in the $5.2 \leqslant H \leqslant 6.5$ MJ $\cdot$ kg^{-1} range.

Figure 3 represents the longitudinal sound velocity c as a function of the density ρ for both solid and liquid beryllium. The density values are calculated from the following expression:

$$\rho = \rho_0 V_0 / V \tag{10}$$

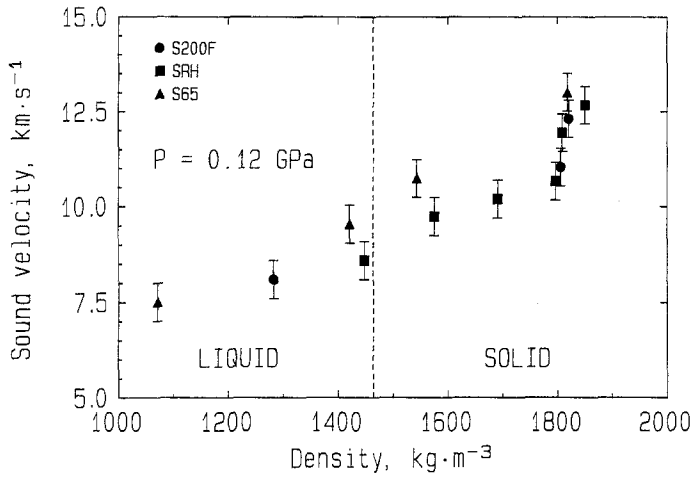

Fig. 3. Sound velocity versus density for both solid and liquid beryllium. The density data are calculated from Eq. (10), where $\rho_0 = 1850\,\mathrm{kg \cdot m^{-3}}$ (see text). The average error estimates of the sound velocity are $\pm 500\,\mathrm{m \cdot s^{-1}}$. The vertical dashed line corresponds to the density of liquid beryllium at the melting point.

V_0/V being deduced from volume expansion measurements and where ρ_0 is the density at 300 K, i.e., $1850\,\mathrm{kg \cdot cm^{-3}}$ (such a value has been measured in our laboratory and is commonly used in the literature). It may be noted that our values are significantly lower than the static data at higher temperatures [19]. For example, the liquid density at the melting point is reported to be $1690\,\mathrm{kg \cdot m^{-3}}$ in Ref. 19, whereas Eq. (10) gives a $1464\,\mathrm{kg \cdot m^{-3}}$ value from our volume measurements.

The most striking facts of these results may be summarized as follows.

(i) As has been observed for most of the materials, sound velocity monotonously increases with density and thus decreases with temperature.

(ii) The very high sound velocity of solid beryllium at $\rho_0 = 1850\,\mathrm{kg \cdot m^{-3}}$ (e.g., 300 K), located in the 12,500–13,000 $\mathrm{m \cdot s^{-1}}$ range, is in very good agreement with the 12,600 $\mathrm{m \cdot s^{-1}}$ value reported in the literature [20]. In the liquid state, the average value is about 8000 $\mathrm{m \cdot s^{-1}}$. To our knowledge, this is the first sound velocity measurement reported for liquid beryllium.

(iii) There is no significant change in the sound velocity at the melting point, as was observed several times for materials such as indium, molybdenum, and iron [21, 22, 23] from sound velocity-versus-temperature curves.

(iv) The sound velocity seems to change notably as a function of the nature of the sample. Indeed, the S65 specimen presented higher values than those for S200F and SRH, although they are still included in our experimental error estimates. As was mentioned before, a scatter in the data was also observed for other physical properties for different kinds of beryllium samples and was attributed principally to impurities in the samples. However, such an assumption does not explain the similar behavior of the SRH and S200F samples, since there is a large difference in degree of purity between these samples (see above). Another explanation could come from the presence of a texture in S200F and SRH samples, the S65 samples being very low in such crystalline defects because of the use of the HIP process. It may also be noted that SRH samples are probably more subject to the presence of texture since they are extracted by an extrusion process. This will be further investigated in the future.

(v) The curve in Fig. 3 shows a behavior similar to that of lead [9, 24], tantalum [25], molybdenum [22, 26], and tungsten [27] since one observers a linear function in the liquid state. Such a dependence is not so obvious in the solid phase.

Concerning the liquid phase, the best least-squares fit to our data is

$$c = 4.23\rho + 2905 \tag{11}$$

where c is in $\mathrm{m \cdot s^{-1}}$ and ρ is in $\mathrm{kg \cdot m^{-3}}$.

4. DISCUSSION

One of the aims of the IEX is to determine partially the equation of state of elements. As mentioned earlier, the knowledge of the sound velocity of the material may give access to the equation-of-state parameters such as the bulk moduli, the Grüneisen coefficient, and the specific heat ratio.

For example, by taking our highest temperature value (2900 K), where $c \approx 7500\ \mathrm{m \cdot s^{-1}}$ and $\rho = 1071\ \mathrm{kg \cdot m^{-3}}$, Eqs. (1)–(6) lead to the following results:

$$B_S = 60.2\ \mathrm{GPa}, \qquad K_S = 1.7 \times 10^{-2}\ \mathrm{GPa^{-1}}$$
$$B_T = 30.1\ \mathrm{GPa}, \qquad K_T = 3.3 \times 10^{-2}\ \mathrm{GPa^{-1}}$$
$$\gamma_G = 2.4, \qquad \gamma = 2$$

where the values $C_p = 3.5\ \mathrm{kJ \cdot kg^{-1} \cdot K^{-1}}$ and $\beta = 1.5 \times 10^{-4}\ \mathrm{K^{-1}}$ have been used for liquid beryllium. Such data have been obtained from our $H = f(T)$

and $V/V_0 = f(T)$ experimental curves, respectively, the latter being collected from one shot with a S200F sample devoted only to pyrometry measurements. These data are in reasonable agreement with the $C_p = 3.3\,\mathrm{kJ \cdot kg^{-1} \cdot K^{-1}}$ [12] and $\beta = 1.16\,10^{-4}\,\mathrm{K^{-1}}$ [19] reported in the literature.

The error calculations on the above parameters may be investigated. Indeed, by considering the ± 7 and $\pm 4\%$ average experimental uncertainties for sound velocity and volume measurements, respectively, the error estimate of B_S is then $\pm 18\%$ since one neglects the error on the ρ_0 density value. Such large error bars give trends and approximative quantitative data to obtain the equation of state of the element.

5. CONCLUSION

The measurements were hard to perform since we encountered numerous experimental difficulties (vaporization of the material, hazy shadow contours, breakable material, etc.). Three kinds of samples were tested, whose experimental data seem to display significant changes as a function of the nature of the sample.

To our knowledge, we report for the first time sound velocity measurements in liquid beryllium. These data show a linear variation with density as was already observed for several materials, on one hand, and no break in these data has been displayed at the melting point, on the other hand.

ACKNOWLEDGMENTS

We would like to thank D. Mauge for providing the beryllium samples. The authors are grateful to A. Berthault, J. P. Le Fauconnier, and J. L. Truffier for their helpful discussions.

REFERENCES

1. O. Kubashewski, *Atomic Energy Review, Vol. 4* (International Atomic Energy agency, Vienna, 1973).
2. A. J. Stonehouse, J. A. Carrabine, and W. W. Beaver, in *Beryllium: Its Metallurgy and Properties*, H. H. Hausner, ed. (University of California, 1965).
3. Y. S. Touloukian, *Thermophysical Properties of High Temperature Solid Materials, Vol. 1, The Elements* (Macmillan, New York, 1967).
4. N. P. Pinto, in *Beryllium Science and Technology*, D. R. Floyd and J. W. Lowe, eds. (Plenum Press, New York and London, 1977), p. 341.
5. S. V. Levedev, A. I. Savvatimskii, and Y. B. Smirnov, *High Temp. High Press.* **9**:578 (1971).
6. G. R. Gathers, J. W. Shaner, and D. A. Young, *Phys. Rev. Lett.* **3**:70 (1974).
7. A. Berthault, L. Arles, and J. Matricon, *Int. J. Thermophys.* **7**:167 (1986).

8. G. R. Gathers, J. W. Shaner, C. A. Calder, and W. W. Wilcox, in *Proc. 7th Symp. Thermophys. Prop.* (ASME, New York, 1977), pp. 904–909.
9. R. S. Hixson, M. A. Winkler, and J. W. Shaner, *High Temp. High Press.* **17**:267 (1985).
10. J. A. Brammer and C. M. Percival, *Exp. Mech.* **10**:245 (1970).
11. C. A. Calder and W. W. Wilcox, *Rev. Sci. Instrum.* **45**:1557 (1974).
12. A. C. Tam, *Rev. Mod. Phys.* **58**:381 (1986).
13. C. B. Scruby, *Appl. Phys. Lett.* **48**:100 (1985).
14. A. M. Aindow, R. J. Dewhurst, D. A. Hutchins, and S. B. Palmer, *J. Acoust. Soc. Am.* **69**:449 (1981).
15. A. N. Nominé and J. P. Le Fauconnier, *Chocs, Rev. Sci. Tech. Appl. Milit. (Comm. Energ. Atom.)* **6**:43 (1992).
16. J. Ho and E. S. Wright, *Electrical Resistivity of Beryllium*, General Research in Materials and Propulsion, Metallurgy and Chemistry, Vol. II (1960).
17. L. V. Gurvich, *Thermodyn. Prop. Ind. Subst.* **3**:230 (1981).
18. G. R. Gathers, *Int. J. Thermophys.* **11**:693 (1990).
19. A. V. Grosse and J. A. Cahill, *ASM Trans. Q. (USA)* **57**:739 (1964).
20. C. B. Sawyer and B. R. F. Kjellgren, *Met. Alloys* **11**:163 (1940).
21. H. Kamioka, *J. Phys. Soc. Jap.* **52**:2784 (1983).
22. R. S. Hixson, D. A. Boness, and J. W. Shaner, *Phys. Rev. Lett.* **62**:637 (1989).
23. J. Brown and R. G. McQueen, *J. Geophys. Res.* **91**:7485 (1986).
24. R. S. Hixson, M. A. Winkler, and J. W. Shaner, *Physica* **139, 140B**:893 (1986).
25. R. S. Hixson, M. A. Winkler, and J. W. Shaner, *High Temp. High Press.* **18**:635 (1986).
26. R. S. Hixson and M. A. Winkler, *Int. J. Thermophys.* **13**:477 (1992).
27. R. S. Hixson and M. A. Winkler, *Int. J. Thermophys.* **11**:709 (1990).